First published in: Proceedings / 18. Symposium Simulationstechnique, Erlangen, September 12-15, 2005. Erlangen, 2005. ISBN 3-936150-41-9

A coupled 3D Simulator for Solidification Microstructures with Fluid Flow

Michael Selzer*, Britta Nestler†, Frank Wendler‡
Faculty of Computer Science
Karlsruhe University of Applied Sciences
Moltkestrasse 30
D-76133 Karlsruhe, Germany

Abstract

We present a new phase-field model with fluid flow which has the capability of studying the effect of fluid flow on crystal growth structures by numerical simulations. The model contains a set of phase-field equations describing the evolution of the phase states in the system coupled with the Navier-Stokes equations for fluid flow. The recently developed simulator for solving these equations is based on a finite difference method on a rectangular staggered grid. The pressure and the phase state variables are located in the cell centers whereas the three-dimensional velocity components are computed in the midpoints shifted by half a grid spacing of the three types of cell edges parallel to the coordinate axes. To improve the efficiency of the code, we use adaptive algorithms and parallelization techniques to perform the iterations. The time discretization is accomplished by an implicit successive overrelaxation (SOR) method for the pressure iteration and an explicit scheme for updating all other variables. Numerical results of Couette flow across a planar solid-liquid solidification front and of flow around particles with diffuse interfaces are discussed.

1 Introduction

From experiments, it is well known that fluid flow has a great influence on the solidification structure during a casting process. The presence of flow admits the possibility of instabilities due to the flow itself, in addition to the morphological instabilities normally found in crystal growth. Hence, flow has an important influence on the process conditions and on the resulting material properties during the solidification from a melt. It is an inherently three-dimensional phenomenon where solute is transported in the spatial domain and around the growing crystals.

In the research field of modelling solidification microstructures in 3D, the phase-field formalism has become of great importance. The introduction of a diffuse phase-field variable with a smooth transition at a phase boundary enables the numerical computation of complex structures such as dendrites and multiphase structures for the first time. In [1], the growth of dendrites with and without fluid flow was simulated on the basis of a phase-field approach. The power of the methodology lies in its computational applicability leading to new and advanced insights in the processes of pattern formation.

*semi0016@hs-karlsruhe.de
†britta.nestler@hs-karlsruhe.de
‡frank.wendler@hs-karlsruhe.de

We extend a recently formulated phase-field model for multiphase systems in [2] to describe the influence of fluid flow on the microstructure evolution. The equations of motion are solved numerically by using finite differences on a staggered grid, parallel and adaptive algorithms to improve the efficiency of the solver. The model is summarized in Sec. 2 and the discretization is described in Sec. 3 followed by an illustration of a flow chart of the code structure in Sec. 4. We complete the paper with two examples of fluid flow at solid-liquid interfaces.

2 Phase-field model with fluid flow

To treat crystal growth under the influence of convection, as is inevitable in realistic solidification environments, a coupling of the phase-field model and fluid dynamics must be realized. We restrict the problem to quasi-incompressibility, where the density of the fluid (melt), in which the growing crystal evolves, does not depend on pressure, but may depend on concentration or temperature. The basic idea is to describe the crystal not as an external obstacle but as a fluid with a viscosity 50 - 500 times higher as compared to the melt. Therefore, a space depending viscosity parameter $\mu(\phi)$ is introduced, which averages the two phase dependant values of the viscosity over the diffuse interface using two strategies with different numerical stability:

$$\mu(\phi) = \sum_{\alpha=1}^{N} \mu_\alpha \phi_\alpha \quad \text{(arithmetic)} \tag{1}$$

$$\text{or} \quad \frac{1}{\mu(\phi)} = \sum_{\alpha=1}^{N} \frac{\phi_\alpha}{\mu_\alpha} \quad \text{(harmonic)} \tag{2}$$

Here, μ_α is the viscosity of phase α and the variable ϕ is a vector-valued order parameter $\phi = (\phi_1, \ldots, \phi_N)$, where each component ϕ_α represents the phase state or grain orientation of a certain phase or grain in the system. The phase-fields $\phi_\alpha, \alpha = 1, \ldots, N$ take the values $\phi_\alpha \in \{0, 1\}$ in the bulk phases with a smooth transition in the region of a diffuse interface thickness of width ε. Following an ansatz formerly published in [3, 4], a thermodynamically consistent multi-phase-field model including the incompressible Navier-Stokes equations was derived. The model is based on a total entropy formulation of a material volume $\Omega(t)$, given by

$$\mathcal{S} = \int_{\Omega(t)} \Big[\rho s(\phi) - \big(\varepsilon\, a(\phi, \nabla\phi) + \frac{1}{\varepsilon}\, w(\phi) \big) \Big] dV,$$

where ρ is the density and s the bulk entropy per mass unit. The second and thrid term in round brackets represent all surface contributions and include the diffuse interface width ε, the anisotropic gradient entropy density $a(\phi, \nabla\phi)$ and the multi-well potential $w(\phi)$ inherent to phase-field modelling. The physical laws of conservation of linear momentum, mass, internal energy and the second law of thermodynamics (positive entropy production) can be formulated as volume integrals and can be recasted into partial differential equations. This results in the following set of evolution equations for the phase-field (order parameter) variables ϕ_α of all coexisting phases and for the velocity field $\vec{u}$:

$$\tau\varepsilon\frac{D\phi_\alpha}{Dt} = \varepsilon\nabla\cdot\left(\rho\frac{\partial a(\phi,\nabla\phi)}{\partial\nabla\phi_\alpha} - \rho\frac{\partial a(\phi,\nabla\phi)}{\partial\phi_\alpha}\right) - \frac{\rho}{\varepsilon}\frac{\partial w(\phi)}{\partial\phi_\alpha} - \frac{\rho}{T}\frac{\partial f(\phi)}{\partial\phi_\alpha} - \lambda \quad (3)$$

$$\rho\frac{D\vec{u}}{Dt} = \nabla\cdot(\boldsymbol{\sigma} + \boldsymbol{\theta_{cap}}) = \nabla\cdot\left[-p\boldsymbol{I} + \mu(\phi)(\nabla\vec{u} + (\nabla\vec{u})^T) + \boldsymbol{\theta_{cap}}\right] \quad (4)$$

$$\nabla\cdot\vec{u} = 0. \quad (5)$$

Eqs. (4) and (5) represent the modified fully incompressible Navier-Stokes equations. In this context, the transport derivation $D/Dt = \partial/\partial t + \vec{u}\cdot\nabla$ is applied, mass and energy balance equations are omitted. Except for the additional $l.h.s$ advective term of the form $\vec{u}\cdot\nabla\phi_\alpha$, the phase-field equation in Eq. (3) remains unchanged after coupling fluid dynamics. For a comprehensive review of the phase-field model functions see [2]. The Navier-Stokes Eq. (4) is supplemented by the capillary tensor $\boldsymbol{\theta_{cap}}$. The 'classical' part of the stress tensor $\boldsymbol{\sigma}$ contains the pressure p as a driving force of a liquid flow ($\boldsymbol{I}$ denotes the unity matrix) as well as internal friction proportional to the viscosity $\mu(\phi)$. The capillary interfacial forces are represented by $\boldsymbol{\theta_{cap}}$ which are important when dealing with structure dimensions in the micron range; it can be related to the surface entropy density $a(\phi, \nabla\phi)$ in the phase-field model as

$$\boldsymbol{\theta_{cap}} = \left[a(\phi,\nabla\phi)\boldsymbol{I} - \sum_{\alpha=1}^{N}\left(\frac{\partial a(\phi,\nabla\phi)}{\partial(\nabla\phi_\alpha)}\otimes\nabla\phi_\alpha\right)\right], \quad (6)$$

where $\otimes$ denotes the tensor product and the summation extends over the number of all N existing phases in the calculation domain.

3 Discretization

The set of partial differential equations (Eqs. (3)-(5)) is solved numerically by using a finite difference discretization on a staggered grid, in which the different variables are located at different grid points. The iteration of the Poisson equation for the pressure is accomplished applying a successive overrelaxation method (SOR). As illustrated in Fig. 1 in 2D, the components of the velocity $\vec{u}_{i,j} = (u_{i,j}, v_{i,j})$ are located in the midpoints of the cell edges, the phase fields $\phi^\alpha_{i,j}$ and the pressure in the center of a cell. In 3D, the phase fields $\phi^\alpha_{i,j,k}$ are computed in the center of a cell-cube and the velocity components $\vec{u}_{i,j,k}$ are located in the center of the analogical side-area.

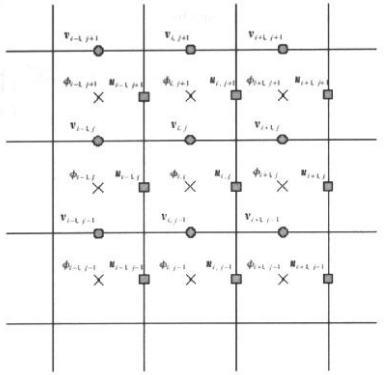

Figure 1: Location of the values on a staggered grid in 2D.

In the following, we exemplarily describe the discretization of some terms of the Eqs. (3) - (5), particularly relevant for the coupling of phase-field and Navier-Stokes equations. The discretized form of the term $\vec{u}\cdot\nabla\phi_\alpha$ in Eq. (3) lies in the ϕ-grid and reads

$$\vec{u}_{i-\frac{1}{2},j-\frac{1}{2},k-\frac{1}{2}}\cdot\nabla^c\phi^\alpha_{i,j,k} = \begin{pmatrix}\frac{u_{i,j,k}+u_{i-1,j,k}}{2}\\ \frac{v_{i,j,k}+v_{i,j-1,k}}{2}\\ \frac{w_{i,j,k}+w_{i,j,k-1}}{2}\end{pmatrix}\cdot\begin{pmatrix}\frac{\phi^\alpha_{i+1,j,k}-\phi^\alpha_{i-1,j,k}}{2\Delta x}\\ \frac{\phi^\alpha_{i,j+1,k}-\phi^\alpha_{i,j-1,k}}{2\Delta y}\\ \frac{\phi^\alpha_{i,j,k+1}-\phi^\alpha_{i,j,k-1}}{2\Delta z}\end{pmatrix}$$

$$= \frac{1}{4}\left\{\frac{(u_{i,j,k}+u_{i-1,j,k})(\phi^\alpha_{i+1,j,k}-\phi^\alpha_{i-1,j,k})}{\Delta x} + \frac{(v_{i,j,k}+v_{i,j-1,k})(\phi^\alpha_{i,j+1,k}-\phi^\alpha_{i,j-1,k})}{\Delta y} + \frac{(w_{i,j,k}+w_{i,j,k-1})(\phi^\alpha_{i,j,k+1}-\phi^\alpha_{i,j,k-1})}{\Delta z}\right\},$$

where we use mean values for the velocities $\vec{u}_{i-\frac{1}{2},j-\frac{1}{2},k-\frac{1}{2}}$ and central differences for the differential operator $\nabla\phi_\alpha = \nabla^c\phi^\alpha_{i,j,k}$.
The coupling of the Navier-Stokes Eq. (4) with the phase fields involves two terms: the phase dependant viscosity $\mu(\phi)$ in the irreversible viscous stress tensor $\boldsymbol{\tau} = \mu(\phi)(\nabla\vec{u} + (\nabla\vec{u})^T)$ and the capillary tensor $\boldsymbol{\theta_{cap}}$ of Eq. (6). We will demonstrate the discrete form of $\boldsymbol{\tau}$, but, due to its complexity, we refer to a forthcoming paper for the discretization of $\boldsymbol{\theta_{cap}}$, since it involves the gradient entropies $a(\phi, \nabla\phi)$ and anisotropies of the phase-field model.

The divergence of the viscous stress tensor is given by

$$\begin{aligned}\nabla \cdot [\boldsymbol{\tau}] &= \nabla \cdot [\mu(\phi)(\nabla \vec{u} + (\nabla \vec{u})^T)] \\ &= \nabla \cdot \left[\mu(\phi) \begin{pmatrix} 2\partial_x u & \partial_x v + \partial_y u & \partial_x w + \partial_z u \\ \partial_y u + \partial_x v & 2\partial_y v & \partial_y w + \partial_z v \\ \partial_z u + \partial_x w & \partial_z v + \partial_y w & 2\partial_z w \end{pmatrix} \right],\end{aligned}$$

where ∂_x, ∂_y and ∂_z of the velocity components denote the partial derivatives with respect to the coordinates x, y, z, respectively. To discretize $\nabla \cdot [\boldsymbol{\tau}]$, we use forward and backward differences, i.e. $\nabla^l \cdot [\boldsymbol{\tau}^r]$ with

$$\boldsymbol{\tau}^r = \begin{pmatrix} (\mu_{11}(\phi)\tau_{11})^r & (\mu_{12}(\phi)\tau_{12})^r & (\mu_{13}(\phi)\tau_{13})^r \\ (\mu_{21}(\phi)\tau_{21})^r & (\mu_{22}(\phi)\tau_{22})^r & (\mu_{23}(\phi)\tau_{23})^r \\ (\mu_{31}(\phi)\tau_{31})^r & (\mu_{32}(\phi)\tau_{32})^r & (\mu_{33}(\phi)\tau_{33})^r \end{pmatrix}.$$

$\mu(\phi)$ is calculated according to Eqs. (1) and (2). For the arithmetic expression in Eq. (1), we obtain the discrete form of $\boldsymbol{\tau}^r$ matching the staggered grid

$$\begin{aligned}(\mu_{11}(\phi)\tau_{11})^r &= \left(\sum_{\alpha=1}^{N} \mu_\alpha \phi^\alpha_{i+1,j,k} \right) \cdot 2 \left(\frac{u_{i+1,j,k} - u_{i,j,k}}{\Delta x} \right) \\ (\mu_{12}(\phi)\tau_{12})^r &= \left(\sum_{\alpha=1}^{N} \mu_\alpha \phi^\alpha_{i+\frac{1}{2},j+\frac{1}{2},k} \right) \cdot \left(\frac{v_{i+1,j,k} - v_{i,j,k}}{\Delta x} + \frac{u_{i,j+1,k} - u_{i,j,k}}{\Delta y} \right),\end{aligned}$$

where $\phi^\alpha_{i+\frac{1}{2},j+\frac{1}{2},k}$ corresponds to the mean value

$$\phi^\alpha_{i+\frac{1}{2},j+\frac{1}{2},k} = \frac{1}{4} \left(\phi_{i,j,k} + \phi_{i+1,j,k} + \phi_{i,j+1,k} + \phi_{i+1,j+1,k} \right).$$

The other components of the tensor $\boldsymbol{\tau}^r$ can be formulated in an analogous way.

4 Code structure

The phase-field solver and the Navier-Stokes solver are coupled as shown in the flow chart in Fig. 2. The value Δt_n is constant for each simulated time step. For numerical stability, the time step $\Delta t_{n_{NS}}$ is calculated after each iteration of the Navier-Stokes solver. If the next $\Delta t_{n_{NS}}$ exceeds Δt_n, it is reduced to fit.

Early experiments have shown that Δt_n necessary for a stable phase-field solution is greater than $\Delta t_{n_{NS}}$, so that the Navier-Stokes equations need several iterations to match the next Δt_n. This has a big impact on the calculation time. In addition, the SOR-iteration for the Poisson equation needs a lot of CPU-cycles. Further development is needed to parallelize the SOR-iteration with the help of OpenMP and MPI. Both parallelizing mechanisms are already introduced in the phase-field solver and the results of the optimization efforts are successful.

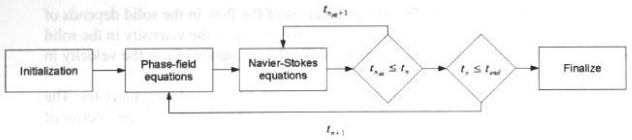

Figure 2: Flow-chart of the coupled phase-field and Navier-Stokes solver.

5 Simulation Results

In this section, the developed phase-field simulator with fluid flow is applied to model the flow field in the presence of diffuse solid-liquid interfaces.

The first example in Fig. 3 is devoted to recover the velocity profile across a planar solid-liquid interface known as Couette flow.

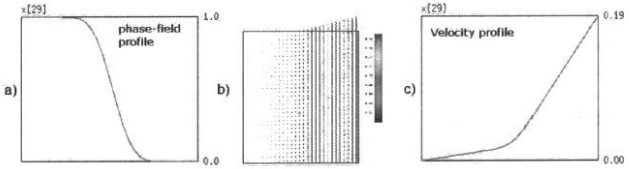

Figure 3: Approximation to Couette flow obtained from a phase-field simulation: a) Image of the diffuse solid-liquid interface, b) stationary flow field in the presence of a moving wall at the right, c) velocity profile across the diffuse interface.

For simplicity, we consider the situation where the system is isothermal and the densities of both the solid phase and the liquid phase are constant and equal. We examine the influence of the kinematic viscosity $\mu(\phi)$ on the flow field. The distinction between the solid and the liquid phase for the flow field is given by their different viscosities: $\mu_S/\mu_L \gg 1$. We take a two-dimensional x/y domain with Nx and Ny grid points coincident with a fixed left wall at $x = 0$. The right wall at $x = Nx \cdot \delta x$ moves with a constant speed in y direction. In- and out-flow conditions are set at the bottom and top of the domain. A planar diffuse solid-liquid interface is located at $x = Nx/2$ parallel to the y-direction and the solid phase is posed in the left half. The simulation result is displayed in Fig. 3 for the case $\mu_S/\mu_L = 10$. Due to the difference in viscosities, the velocity profile has a much smaller slope in the solid than in the liquid. A clear transition can be seen at the position of the interface. The reason for a non-zero velocity in the solid lies in the model assumption that the solid phases

are treated as high viscous liquids. The absolute values of the flow in the solid depends of course on the viscosity parameter μ_S. For the simulation in Fig. 3, the viscosity in the solid was chosen only ten times as large as in the liquid. For larger values of μ_S, the velocity in the solid approaches zero.
In the simulation in Fig. 4, we considered the flow around diffuse and inert particles. The velocity performs local accelerations, and almost no flow can be observed in the interior of the particles.

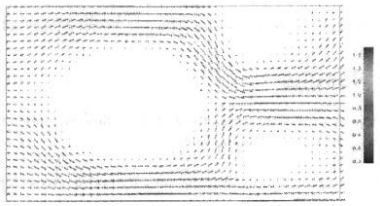

Figure 4: Phase-field simulation of fluid flow around inert particles with a diffuse solid-liquid interface boundary.

Acknowledgements

The authors thank both, the state Baden-Wuerttemberg within the programme LARS, Grand No. lars-08.17 and the German Research Foundation (DFG) within the Prioritiy Research Programme 1095 under Grand No. Ne 822/1-2 for the financial support of this work.

References

[1] *Jeong, J.-H., Goldenfeld, N., Dantzig, J. A.:* Phase-field model for three-dimensional dendritic growth with fluid flow. Phys. Rev. E, Vol. 64 (2001), 041602.

[2] *Garcke, H., Nestler, B., Stinner, B.:* A diffuse interface model for alloys with multiple components and phases. SIAM J. Appl. Math. 64, (2004) 775 - 799.

[3] *Anderson, D. M., McFadden, G. B., Wheeler, A. A.:* A phase-field model of solidification with convection. Physica D 135 (2000), 175-194.

[4] *Nestler, B., Wheeler, A. A., Ratke, L., Stoecker, C.:* Phase-field model for solidification of a monotectic alloy with convection. Physica D 141, (2000) 133 - 154.

Parallel Computing in Applications

Gundolf Haase

Frank Hülsemann